Modal Analysis Based on the Random Decrement Transform

Asmussen, J. C.; Brincker, Rune; Ibrahim, S. R.

Publication date:
1998

Document Version
Publisher's PDF, also known as Version of record

INSTITUTTET FOR BYGNINGSTEKNIK

DEPT. OF BUILDING TECHNOLOGY AND STRUCTURAL ENGINEERING
AALBORG UNIVERSITET • AAU • AALBORG • DANMARK

FRACTURE & DYNAMICS
PAPER NO. 110

To be presented at the Nato Advanced Study Institute on Modal Analysis and Testing, Sesimbra, Portugal, May 3-15, 1998

J. C. ASMUSSEN, R. BRINCKER, S. R. IBRAHIM
MODAL ANALYSIS BASED ON THE RANDOM DECREMENT TRANSFORM
APRIL 1998

ISSN 1395-7953 R9821

The FRACTURE AND DYNAMICS papers are issued for early dissemination of research results from the Structural Fracture and Dynamics Group at the Department of Building Technology and Structural Engineering, University of Aalborg. These papers are generally submitted to scientific meetings, conferences or journals and should therefore not be widely distributed. Whenever possible reference should be given to the final publications (proceedings, journals, etc.) and not to the Fracture and Dynamics papers.

Printed at Aalborg University

MODAL ANALYSIS BASED ON THE RANDOM DECREMENT TRANSFORM

J.C. Asmussen & R. Brincker

Department of Building Technology and Structural Engineering

Aalborg University, Denmark.

S.R. Ibrahim

Department of Mechanical Engineering, Old Dominion University,

Virginia, USA.

ABSTRACT

During the last years several papers utilizing the Random Decrement transform as a basis for extraction of modal parameters from the response of linear systems subjected to unknown ambient loads have been presented. Although the Random Decrement technique was developed in a decade starting from the introduction in 1968 the technique seems still to be attractive. This is probably due to the simplicity and the speed of the algorithm and the fact that the theory of the technique has been extended by introducing statistical measures such as correlation functions or spectral densities. The purpose of this paper is to present a state-of-the-art description of the Random Decrement technique where the statistical theory is outlined and examples are given. But also new results such as estimation of frequency response functions and quality assessment are introduced. Special attention is given to the theoretical background for the application of the Random Decrement transform to ambient measurements.

1. INTRODUCTION

During the last few years several papers concerning application and theory of the Random Decrement (RD) transform have been presented at conferences and appeared as reviewed papers in journals, see references [59-79]. Especially the application of the RD transform to ambient data or the response of linear systems to unknown and unmeasurable forces has been studied and developed. The reason is probably that the RD transform is easily implemented and is a very fast technique to transform data into a form, which immediately can be interpreted by the user. In spite of this not much attention has been given to this transform since its introduction in 1968 compared to e.g. Fourier transformation. Prior to this work the authors could only find about 79 papers, reports, theses etc. concerning both application and theoretical aspects of the RD technique. Most of these papers interprets the results of an RD transform as either free decays or correlation functions. This contradiction is cleared up by showing that the correlation functions have the same shape as free decays.

The purpose of this paper is to give an overview of the RD transform. Special attention is given to the theoretical background for the RD transform applied to ambient measurements. The relation between the RD functions and the free decays of the structures is shown by means of correlation functions and Gaussian processes. These relations are the basis for new methods to formulate an appropriate RD transform and to assess the results of the RD transform. An example of the application of this new method is given by the analysis of ambient measurements of a bridge.

Section 2 gives a short background of the historical development of the RD transform. Both theoretical and application work are considered. In section 3 the RD functions are defined and the estimation algorithm is discussed. The different triggering conditions are described and an example of the application of the RD transform to sinusoidals is given. A new approach for estimation of frequency response functions (FRF) based on the RD transform of the measured input and output is shown together with an example in section 4. The theoretical background for the RD technique applied to ambient measurements is discussed in section 5 by studying linear systems loaded by filtered white noise. In section 6 a new concept, Quality assessment, is introduced. The theoretical results of sections 5 and 6 are applied to ambient measurements of a bridge in section 7. Section 8 describes a recently developed vector formulation of the RD transform. The paper is finished with a conclusion.

2. DEVELOPMENT OF THE RD TECHNIQUE

The RD transform was introduced by H.A. Cole in 1968, Cole [1] and further developed in Cole [2] - [4]. Cole was working with identification of damping and natural frequencies of aerospace structures loaded by unmeasureable flutter. He found that the estimates of the damping ratios by the half-power bandwidth of the spectral densities resulted in too uncertain estimates. Further, he did not have any standard method to detect non-linearities from the spectral densities. Instead he was looking for a method to transform the ambient responses into a form meaningful to the observer, Cole [1].

Cole stated that the stochastic response of a structure at the time $t_0 + t$ is composed of three parts: 1) The step response from the initial displacements at the time t_0. 2) The impulse response from the initial velocity at the time t_0. 3) A stochastic part which is due to the load applied to the structure in the period t_0 to $t_0 + t$. What would happen if a time segment was picked out every time the stochastic response, $x(t)$, has an initial displacement, say $x(t)$=a, and these time segments were averaged? This algorithm was implemented as

$$\hat{D}_{XX}(\tau) \;=\; \frac{1}{N}\sum_{i=1}^{N} x(t_i)x(t_i+\tau)|x(t_i) = a \;, \quad \tau \geq 0 \tag{1}$$

where D_{XX} is denoted the RD function. As the number of averages N increase the stochastic part due to the random load will eventually average out and be negligible. Furthermore, the sign of the initial velocity is expected to vary randomly with time so the resulting initial velocity will be zero. The only part left is the free decay response from the initial displacement, a.

Cole also introduced another formulation. The time segments are picked out if the stochastic response crosses the zero-line with positive slope. The resulting RD functions were interpreted as an impulse response function.

$$\hat{D}_{XX}(\tau) \;=\; \frac{1}{N}\sum_{i=1}^{N} x(t_i+\tau)|x(t_i) = 0, \dot{x}(_i) > 0 \;, \quad \tau \geq 0 \tag{2}$$

The triggering conditions in equations (1) and (2) are denoted level crossing and zero crossing. The motivation is that the condition is implemented so that a triggering point is detected if the measurement crosses the triggering level and not if it is identical to the triggering level.

The approach Cole used was based on SDOF systems, so the data were filtered prior to the application of the RD algorithm. Cole also used the technique for damage detection in references [3] and [4]. The RD technique was especially applied to flight flutter testing in the following years, see references [5] - [15].

In 1977 the theory of the RD technique was extended to deal with multiple measurements and multiple modes, see Ibrahim [16] and [17]. Firstly, the concept of auto and cross RD functions was introduced and secondly the Ibrahim Time Domain algorithm was used to extract modal parameters from the RD functions equivalent to free decays. The auto, $D_{XX}(\tau)$, and cross, $D_{YX}(\tau)$, RD functions were defined as

$$D_{XX}(\tau) = \frac{1}{N}\sum_{i=1}^{N} x(t_i+\tau)|x(t_i)=a \qquad D_{YX}(\tau) = \frac{1}{N}\sum_{i=1}^{N} y(t_i+\tau)|x(t_i)=a \tag{3}$$

The cross RD were interpreted as free decays with unknown initial conditions, but with contribution from the loads averaged out with an increasing number of averages. For e.g. n measurements the RD technique could transform the measurements into free decays from which multiple modes could be estimated using ITD. Examples of the application to the linear systems loaded by processes with different spectral densities are given in Ibrahim [21,22].

Although the RD technique worked well due to the theoretical extension described above and was applied to several problems, e.g. damage detection, see references [18,19,23,24,30,32-34,38-40], and real data, see references [25,26,35-37,41,42], a disadvantage of the technique was the lack of a statistical background. This would make the technique comparable with the results of Fourier transformation applied to ambient data. Furthermore, there was no description of what would happen if the time segments were also picked out for negative time lags. The answer to this problem was solved in 1982 by Vandiver et al. [27]. They proved that if $X(t)$ is a zero mean Gaussian distributed ergodic process, the RD function obtained using level crossing of the process would be proportional to the correlation function of $X(t)$.

$$D_{XX}(\tau) = \frac{R_{XX}(\tau)}{\sigma_X^2}\cdot a \tag{4}$$

By assuming that the time segments in the averaging process were uncorrelated the variance of the estimate of the RD functions could be predicted as

$$\mathrm{Var}(\hat{D}_{XX}(\tau)) = \frac{\sigma_X^2}{N}\left(1-\left(\frac{D_{XX}(\tau)}{\sigma_X^2}\right)^2\right) \tag{5}$$

This result is important, although it does not change the algorithms directly. Firstly, negative time lags can be understood theoretically and used, and secondly, due to the Wiener-Khintchine relations, there is a direct relation for the results of the RD technique and the results of the FFT algorithm in the form of spectral densities.

This result will be the starting point of this paper. The idea introduced by Vandiver has been used for further development and investigation, see references [46-53,56,60,62-65,67,69,70,72,74-80]. In the following two sections the auto and cross RD functions will be defined using conditional mean values and linked to the correlation functions of Gaussian processes.

3. DEFINITION AND ESTIMATION OF RD FUNCTIONS

Consider two variables $X(t)$ and $Y(t)$. At this stage it is not necessary to assume anything about the statistical nature of the variables, such as e.g. stationarity, ergodicity or probability distribution. $X(t)$ and $Y(t)$ could even be deterministic or non-stationary. The auto, $D_{XX}(\tau)$, $D_{YY}(\tau)$, and cross, $D_{XY}(\tau)$, $D_{YX}(\tau)$, RD functions are defined as

$$\begin{bmatrix} D_{XX}(\tau) & D_{XY}(\tau) \\ D_{YX}(\tau) & D_{YY}(\tau) \end{bmatrix} = \begin{bmatrix} \mathrm{E}[X(t+\tau)|T_{X(t)}] & \mathrm{E}[X(t+\tau)|T_{Y(t)}] \\ \mathrm{E}[Y(t+\tau)|T_{X(t)}] & \mathrm{E}[Y(t+\tau)|T_{Y(t)}] \end{bmatrix} \tag{6}$$

The time variable τ can be both positive and negative corresponding to the time variable in correlation functions of stationary processes. As seen the number of RD functions for a series of variables, say n corresponds to the number of correlation functions, n^2. The conditions $T_{X(t)}$ and $T_{Y(t)}$ are denoted triggering conditions. The different RD functions in the RD matrix are linked together columnwise by the triggering condition.

The RD matrix is estimated as the empirical mean value

$$\begin{bmatrix} \hat{D}_{XX}(\tau) & \hat{D}_{XY}(\tau) \\ \hat{D}_{YX}(\tau) & \hat{D}_{YY}(\tau) \end{bmatrix} = \begin{bmatrix} \frac{1}{N_x}\sum_{i=1}^{N_x} x(t_i+\tau)|T_{x(t_i)} & \frac{1}{N_y}\sum_{i=1}^{N_y} x(t_i+\tau)|T_{y(t_i)} \\ \frac{1}{N_x}\sum_{i=1}^{N_x} y(t_i+\tau)|T_{x(t_i)} & \frac{1}{N_y}\sum_{i=1}^{N_y} y(t_i+\tau)|T_{y(t_i)} \end{bmatrix} \tag{7}$$

If $X(t)$ and $Y(t)$ are ergodic stochastic processes the above equations provide unbiased estimates of the RD functions. The number of triggering points N_x and N_y are determined by the length of $x(t)$ and $y(t)$ and the triggering conditions $T_{X(t)}$ and $T_{Y(t)}$.

From equations (6) and (7) it becomes clear that the main advantages of the RD transform is the simplicity of the implementation of the estimation algorithm and the speed, since only detection of triggering points and averaging of time segments are necessary. In general the main problem in the application of the RD transform is the formulation of the triggering condition, since the formulation for a given length of the realizations is decisive for the number of triggering points.

3.1. TRIGGERING CONDITIONS

Several different formulations of the triggering conditions have been applied. The four most well-known triggering conditions are level crossing, T^L, local extremum, T^E, banded positive, T^P, and zero crossing with positive slope, T^Z. The different triggering conditions can be formulated as

$$\begin{aligned} T^L_{X(t)} &= \{X(t) = a\} & T^E_{X(t)} &= \{a_1 \leq X(t) < a_2, \dot{X}(t) = 0\} \\ T^P_{X(t)} &= \{a_1 \leq X(t) < a_2\} & T^Z_{X(t)} &= \{X(t) = 0, \dot{X}(t) > 0\} \end{aligned} \tag{8}$$

Figure 1 shows a time series where the triggering points selected by the above triggering conditions are shown together with the size of the window in the averaging process used for the first triggering point.

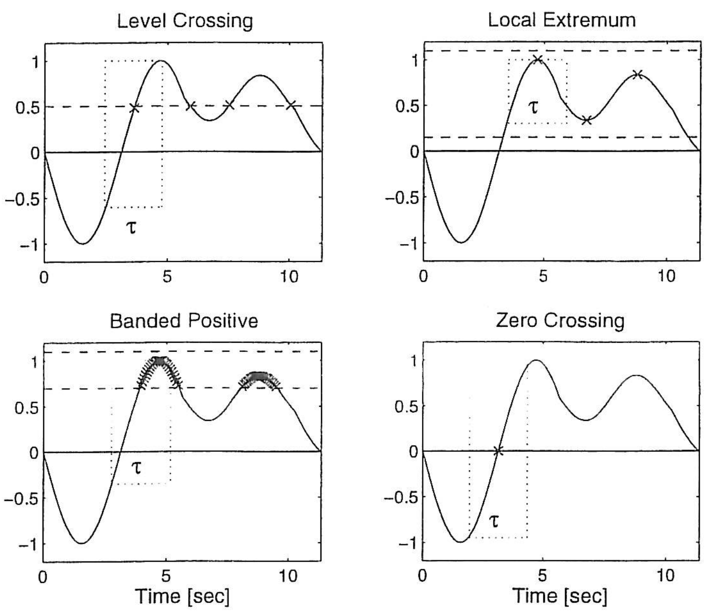

Figure 1: *4 different triggering conditions applied to a continuous time series. The × indicates the triggering points and the dotted box indicates the extent of the time segment (τ). The dashed line indicates the triggering level(s).*

The major differences between the results of the triggering conditions are the shape of the RD functions and the number of triggering points. The most versatile of the four triggering conditions is the banded positive condition, since in the limit $a_1 \approx a_2$ the level crossing triggering condition is obtained.

To illustrate the differences in the number of triggering points an SDOF system loaded by white noise is considered. The natural frequency is 1 Hz, the damping ratio is 1 % and the process is sampled at

10 Hz. The response becomes Gaussian distributed and therefore the expected number of triggering points can be calculated using Rice's formula for the number of level crossings. The expected number of triggering points for the 4 different triggering conditions are shown in figure 2. The upper triggering levels a_2 are taken as ∞ and the lower triggering level, a_1 is varied from 0 to ∞. For the level crossing triggering condition $a_1 = a$. Notice that only the number of triggering points for the banded positive condition is dependent on the sampling rate.

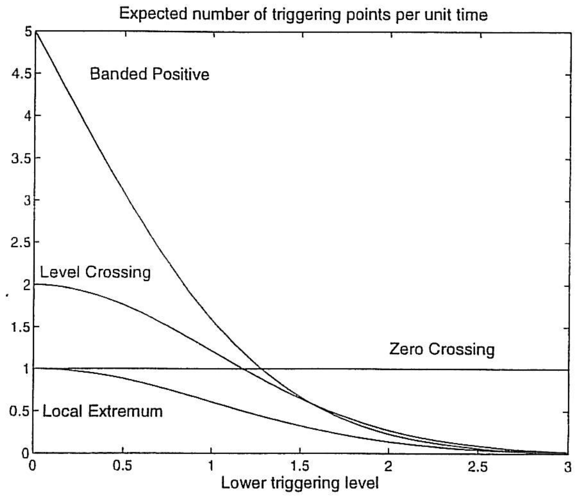

Figure 2: *Expected number of triggering points for 4 triggering conditions for the response of a low-damped SDOF system loaded by white noise and sampled at* $10 \cdot f$.

As seen the expected number of triggering points is highly dependent on the choice of triggering levels. In order to generalize the RD technique a general applied triggering condition, T^{G_A} has been introduced.

$$T^{G_A}_{X(t)} = \{a_1 \leq X(t) < a_2, b_{\leq}\dot{X}(t) < b_2\} \tag{9}$$

The advantage of this condition is that all known particular triggering conditions can be formulated from the above condition. As an example, the level crossing triggering condition can be formulated by $a_1 = a$, $a_2 = a + \Delta a$, $\Delta a \rightarrow 0$ and $[b_1\ b_2] = [-\infty\ \infty]$. The triggering levels should have equal sign.

In application of the RD technique it is common to use *opposite* triggering conditions in order to obtain more triggering points. For e.g. the level crossing condition the following two conditions can be applied.

$$T^L_{X(t)} = a\ , \quad T^L_{X(t)} = -a \tag{10}$$

The two resulting RD functions are subtracted in order to obtain an average estimate of the RD functions.

3.2. EXAMPLE: UNDAMPED AND DAMPED SINUSOIDALS

Consider two sinusoidals. An undamped with frequency 1 Hz and a damped with frequency 1 Hz and damping ratio 2%, see the left-hand part of figure 3. The level crossing triggering condition is applied to both time series with a=0.1 and $\tau \in [-5; 5]$ s. The resulting RD functions are shown in the right-hand part of figure 3.

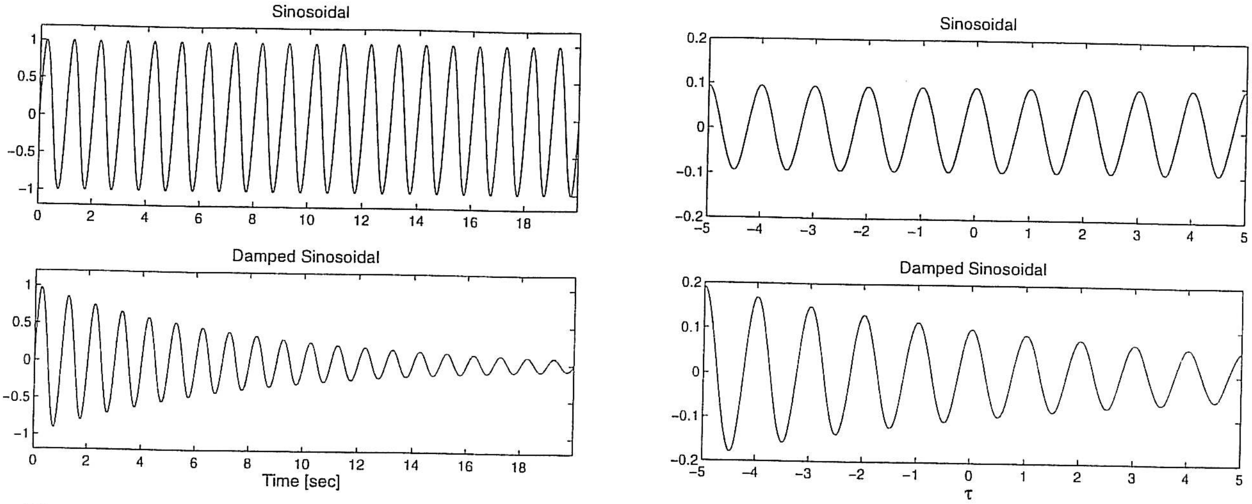

Figure 3: *RD functions of undamped and damped sinusoidals applying level crossing triggering.*

As seen the frequency of the sinusoidals are preserved together with the damping ratio of the damped sinusoidal. The amplitudes have changed and the phase is shifted. This has been proven mathematically in Natke [53].

4. ESTIMATION OF FREQUENCY RESPONSE FUNCTIONS

Two ergodic stochastic processes $X(t)$ and $Y(t)$ are considered. These processes describe the input and output of a linear system. The response of the system is given by the convolution integral

$$Y(t) = \int_{-\infty}^{t} h(t-\eta)X(\eta)d\eta \tag{11}$$

where the influence of the initial conditions has been neglected. Substituting variables, $t = t + \tau$ and $\eta = \xi + t$, eq. (11) can be rewritten as

$$Y(t+\tau) = \int_{-\infty}^{\tau} h(\tau-\xi)X(t+\xi)d\xi \tag{12}$$

Taking the conditional mean value of equation (12) yields

$$\mathrm{E}[Y(t+\tau)|T_X^{G_A}(t)] = \int_{-\infty}^{\tau} h(\tau-\xi)\mathrm{E}[X(t+\xi)|T_X^{G_A}(t)]d\xi \tag{13}$$

or

$$\mathrm{E}[Y(t+\tau)|T_Y^{G_A}(t)] = \int_{-\infty}^{\tau} h(\tau-\xi)\mathrm{E}[X(t+\xi)|T_Y^{G_A}(t)]d\xi \tag{14}$$

Using the definition of the RD functions introduced in section 3 equations (13) and (14) become

$$D_{YX}(\tau) = \int_{-\infty}^{\tau} h(\tau-\xi)D_{XX}(\tau)d\xi \qquad D_{YY}(\tau) = \int_{-\infty}^{\tau} h(\tau-\xi)D_{XY}(\tau)d\xi \tag{15}$$

Equation (15) establishes relations for estimating the impulse response function. The original processes are transformed into the RD functions, but the input-output relation is preserved. The advantage is that noise has been averaged out in the estimation process of the RD functions. Also, the size of the problem has been reduced, since RD functions contain a considerably smaller number of points corresponding to the original time series. If the response of a structure was measured at several points the relation in equation (15) could be extended to cross RD functions only. By introducing the Fourier transform of an RD function as $Z_{XY}(\omega)$ defined as

$$Z_{XY}(\omega) = \frac{1}{2\pi}\int_{-\infty}^{\infty} e^{-i\omega\tau} D_{XY}(\tau) d\tau \tag{16}$$

equation (15) can be transformed into the frequency domain as

$$Z_{YX}(\omega) = H(\omega) Z_{XX}(\omega) \qquad Z_{YY}(\omega) = H(\omega) Z_{XY}(\omega) \tag{17}$$

These two equations constitute a basis for estimating $H(\omega)$ corresponding to e.g. H_1 and H_2 estimators.

$$H(\omega) = H_1^{RD} = \frac{Z_{YX}(\omega)}{Z_{XX}(\omega)} \qquad H(\omega) = H_2^{RD} = \frac{Z_{YY}(\omega)}{Z_{XY}(\omega)} \tag{18}$$

A coherence function for the results of the RD transform can be defined in the frequency domain as

$$\gamma_{xy}^2 = \frac{H_1^{RD}}{H_2^{RD}} = \frac{Z_{XY}(\omega) Z_{YX}(\omega)}{Z_{XX}(\omega) Z_{YY}(\omega)} \tag{19}$$

Equation (19) is only based on two different estimates in the frequency domain. The averaging process is performed in time domain. Alternatively the coherence function for the estimates based on the RD technique could be based on several RD functions estimated with different triggering levels.

It will now be assumed that the load is Gaussian white noise. This means that the response will also be Gaussian distributed. It also means that the RD functions will be proportional to the correlation functions of the processes. Since $R_{YX}(\tau)$, $R_{XY}(\tau)$, $R_{YY}(\tau)$ and $R_{XX}(\tau)$ all satisfy $R \rightarrow 0$ for $|\tau| \rightarrow \infty$ it follows that all RD functions in equation (15) dissipate towards zero with increasing time distance from zero. The result of this relation is that the bounds in the Fourier transformation do not have to be $-\infty$ and ∞ which opens an opportunity to remove leakage errors. This assumes that $R(\pm\tau_{\max}) \approx 0$, where $\tau_{\max}$ is the maximum time lag in the RD function.

Assume that the input to the system is measured by a noise process, U(t), added. The noise process is assumed to be Gaussian distributed and uncorrelated with the measured output, which is free of noise. Subscript M denotes the measured realizations of the different processes

$$y_M = y(t) \,, \quad x_M = x(t) + u(t) \tag{20}$$

The RD functions are proportional to the correlation functions, since the processes are Gaussian distributed

$$R_{Y_M Y_M}(\tau) = E[y_M(t+\tau) y_M(t)] = R_{YY}(\tau) \tag{21}$$

$$R_{X_M Y_M} = E[y_M(t+\tau) x_M(t)] = R_{XY}(\tau) + R_{UY}(\tau) = R_{XY}(\tau) \tag{22}$$

In this situation the estimation of the FRF should be based on H_1^{RD}. Correspondingly if a Gaussian distributed noise process is added to the output of the system and the measured input is noise free the estimation of the FRF should be based on H_2^{RD}.

Two main advantages are expected using the RD based method for estimation of FRF compared to the traditional method based on pure FFT. The computational time is expected to decrease, since the estimation of RD functions only involved averaging, whereas the estimation using pure FFT involves multiplication. In general this question cannot be answered since the estimation time for the RD technique depends on the statistical description of the processes. RD functions are estimated unbiased and dissipate towards zero for increasing absolute time lags. This is an advantage since no leakage errors are introduced.

This new approach could be used in e.g. testing of linear structures using a shaker. The RD functions of the input and output could be sampled continuously. When the RD functions have decayed sufficiently, the experiment is stopped and the FRF/IRF can be estimated.

4.1. EXAMPLE - SDOF LOADED BY WHITE NOISE

Consider an SDOF system with an eigenfrequency $f = 1$ Hz and a low damping ratio of $\zeta = 0.6\%$. The system is loaded by Gaussian white noise. The measurements consist of 40000 points sampled at 5.8 Hz. The FRF is calculated using the traditional method based on the FFT algorithm and the H_1 estimator. 1024 points are used in each time segment for each Fourier transformation and each time segment is multiplied by the Hanning window. The FRF is also estimated using the H_1^{RD} estimator. The positive point triggering condition is used with 1024 points in each RD function and the triggering bounds are chosen as $[a_1\ a_2] = [0.5\sigma_X\ \infty]$. From the FRFs the IRFs are calculated using inverse FFT. The eigenfrequencies and the damping ratios are estimated from the IRFs using the Ibrahim Time Domain algorithm. In order only to have bias errors the modal parameters are estimated using the two approaches from 100 independent simulations of the Gaussian white noise load and the corresponding response. Figure 4 shows a typical auto and cross RD function for the Gaussian white noise load, $D_{XX}(\tau)$, and the response, $D_{YX}(\tau)$.

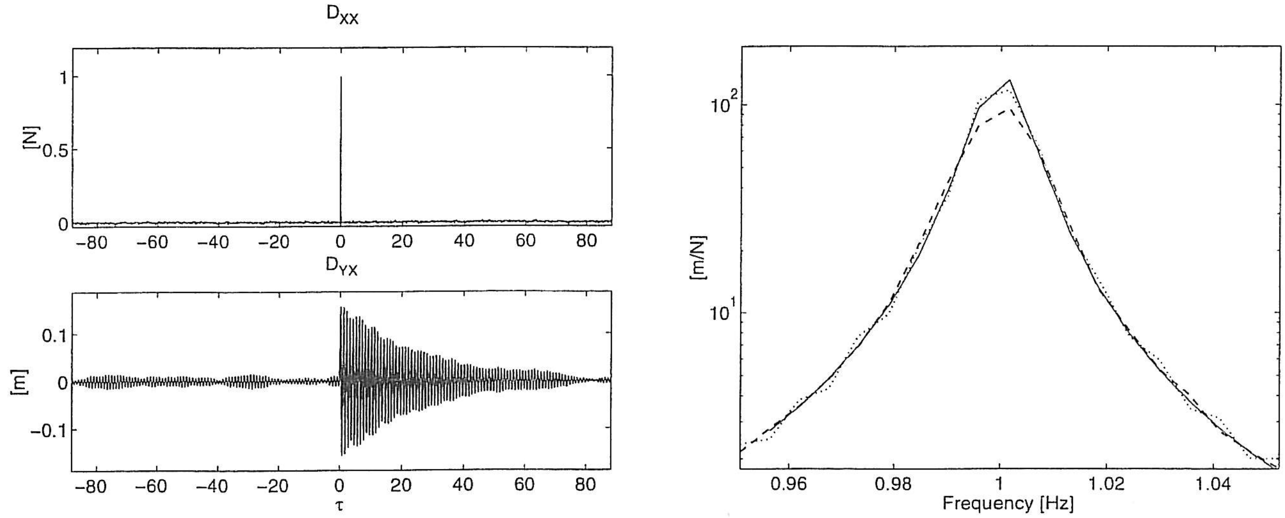

Figure 4: *Typical estimates of the RD functions and zoom of absolute value of the FRFs. [——]: Theoretical. [- - - -]: FFT Hanning window, H_1. [· · · ·]: RD-FFT, No windowing, H_1^{RD}.*

The RD functions dissipate towards zero with increasing time lags. At this stage it might be an advantage to apply an exponential window to the measurements in order to suppress the influence of noise. The right hand part of figure 4 shows a zoom of the FRFs around the resonant frequency.

The increase of the record length has increased the accuracy of the H_1^{RD} estimate, but the H_1 estimate is still biased (an increase in the length of the time segments from 1024 to 2048 would decrease the bias, but increases the random errors).

The estimation of the FRFs using the 5 different approaches is performed 100 times. The mean values and the standard deviations are shown in table 1.

	f [Hz]	σ_f	ζ [%]	σ_ζ
FFT - 40000 pts.	1.000	$0.53\cdot10^{-4}$	0.67	0.0026
RD - 40000 pts.	1.000	$2.69\cdot10^{-4}$	0.60	0.0032

Table 1: *Average values of the modal parameters and the corresponding standard deviations based on 100 simulations. The theoretical values are $f = 1$ Hz and ζ=0.6 %.*

The results show that all approaches provide unbiased estimates of the eigenfrequencies, but the FFT approach provides biased estimates of the damping ratio. On the other hand, the standard deviation of the estimates using the RD technique is higher than the estimates using the FFT approach. If no window function is applied and the system has low damping the ragged spectral densities will result in modal parameters affected by high random errors. The high standard deviations of the modal parameters estimated based on the RD technique is a result of the difficulties which arise in the Fourier transformation of the RD functions.

5. APPLICATION TO LINEAR SYSTEMS LOADED BY WHITE NOISE

In modal analysis the structures are assumed to be linear. If such structures are excited by Gaussian forces the response will also be Gaussian distributed. If the RD transform is applied to Gaussian processes a unique relationship between the RD functions and the correlation functions exist. Consider the general applied triggering condition, see equation (9). If this condition is applied to two jointly distributed Gaussian processes $X(t)$ and $Y(t)$ the following relation can be proven, see [79,71,55,27].

$$D_{XX}(\tau) = \frac{R_{XX}}{\sigma_X^2}\cdot\tilde{a} - \frac{R'_{XX}}{\sigma_{\dot{X}}^2}\cdot\tilde{b} \qquad D_{XY}(\tau) = \frac{R_{XY}}{\sigma_Y^2}\cdot\tilde{a} - \frac{R'_{XY}}{\sigma_{\dot{Y}}^2}\cdot\tilde{b} \tag{23}$$

$$D_{YX}(\tau) = \frac{R_{YX}}{\sigma_X^2}\cdot\tilde{a} - \frac{R'_{YX}}{\sigma_{\dot{X}}^2}\cdot\tilde{b} \qquad D_{YY}(\tau) = \frac{R_{YY}}{\sigma_Y^2}\cdot\tilde{a} - \frac{R'_{YY}}{\sigma_{\dot{Y}}^2}\cdot\tilde{b} \tag{24}$$

$\tilde{a}$ and $\tilde{b}$ are given by

$$\tilde{a} = \frac{\int_{a_1}^{a_2} x p_X(x)dx}{\int_{a_1}^{a_2} p_X(x)dx} \qquad \tilde{b} = \frac{\int_{b_1}^{b_2} \dot{x} p_{\dot{X}}(\dot{x})d\dot{x}}{\int_{b_1}^{b_2} p_{\dot{X}}(\dot{x})d\dot{x}} \tag{25}$$

where $p_X(x)$ and $p_{\dot{X}}(x)$ are the density functions for X and $\dot{X}$, respectively. At the second column of equation (23) the variables in equation (25) should be replaced by Y and $\dot{Y}$. As seen equation (23) establishes a unique relation between the RD transform af Gaussian distributed stochastic processes and their correlation functions.

A linear system with the following governing differential equation is considered

$$\mathbf{M}\ddot{\mathbf{X}}(t) + \mathbf{C}\dot{\mathbf{X}}(t) + \mathbf{K}\mathbf{X}(t) = \mathbf{F}(t) \tag{26}$$

where $\mathbf{M}$, $\mathbf{C}$ and $\mathbf{K}$ are the $n \times n$ mass, damping and stiffness matrices and $\mathbf{F}(t)$ is the force. Traditionally the force is modelled as a white noise vector process. This can be generalized by introducing a shaping filter characterized by its impulse response function $\mathbf{h}^F(t)$.

$$\mathbf{F}(t) = \int_{-\infty}^{t} \mathbf{h}^F(t-\tau)\mathbf{W}(\tau)d\tau \qquad \mathbf{h}(t) = \mathbf{\Phi}_F e^{\mathbf{\Lambda}_F}\mathbf{m}_F^{-1}\mathbf{\Phi}_F^T \tag{27}$$

where $\mathbf{\Phi}_F$ is the mode shapes of the filter, $\mathbf{\Lambda}_F$ is the eigenvalues of the filter and $\mathbf{m}_F$ is a scaling matrix corresponding to modal masses. Using this generalized modelling of the loads it can be shown, see Asmussen [72], that the ith column of the correlation matrix of the response become

$$R_{\mathbf{XX}}(\tau) = \tilde{\mathbf{\Phi}} e^{\tilde{\mathbf{\Lambda}}\tau}\tilde{\mathbf{m}}^{-1}\mathbf{c}_i\ , \quad \tau \geq 0 \qquad R_{\mathbf{XX}}(\tau) = R_{\mathbf{XX}}^T(-\tau) \tag{28}$$

where $\tilde{\mathbf{\Phi}}$, $\tilde{\mathbf{\Lambda}}$ and $\tilde{\mathbf{m}}$ contain mode shapes, eigenvalues and modal masses of the filter and the structure. The concept of the shaping filter was first introduced in Ibrahim [62]. As seen the correlation functions become identical to free decays and thereby can modal parameters be extracted from the correlation functions or RD functions using methods like Ibrahim Time Domain, Polyreference Time Domain, Auto-Regressive Vector models etc. This result was also presented in references [81,82].

The results show a unique relation between the RD transform of Gaussian processes and the modal parameters of a linear system loaded by a generalized white noise driven Gaussian excitation.

6. QUALITY ASSESSMENT

In application of the RD transform the main problem is to select the triggering condition, triggering levels and the size of the time segments, $\tau_{max} - \tau_{min}$ prior to the estimation process. After the estimation process the main question is how to validate the quality of the estimates as a function of different triggering levels and also as a function of the time variable, τ. Two different tests, shape invariance and symmetry test, which can be used to answer the above questions, are suggested. In section 7 the tests are applied to real data.

6.1. SHAPE INVARIANCE TEST

Testing the shape invariance of RD functions is based on several different estimations of a correlation function using different triggering levels for the same triggering condition

$$R^1_{YX}(\tau) = \frac{D_{YX}(\tau)}{a_1}\sigma^2_X \ , \quad R^2_{YX}(\tau) = \frac{D_{YX}(\tau)}{a_2}\sigma^2_X \ , \quad \ldots \tag{29}$$

where superscript $1, 2, \ldots$ refers to the different choice of triggering levels. If different estimates of a correlation function are calculated two different approaches exist to evaluate the shape invariance of the RD functions. First a plot of the different correlation functions is usually sufficient to validate the different estimates of the correlation functions. If a single estimate differs significantly from the rest, the corresponding triggering levels should not be used. If all estimates differ significantly the data should be analysed carefully using the RD technique. So the shape invariance test can also be used in a pre-analysis to select proper triggering levels for a full analysis.

If more than e.g. 5 or 6 different RD functions are estimated it might be difficult to assess the different triggering levels graphically. Instead it is suggested to calculate the correlation between the different RD functions, which will be denoted Shape Invariance Criteria (SIC).

$$\mathrm{SIC}_{R^i_{YX}R^j_{YX}} = \frac{(\sum_{k=1}^{N} R^i_{YX}(k)R^j_{YX}(k))^2}{(\sum_{i=1}^{N} R^i_{YX}(k)^2)(\sum_{k=1}^{N})R^j_{YX}(k)^2} \tag{30}$$

The result of calculating the SIC values between all different estimates of the correlation functions is a matrix with unity in the diagonals. The off-diagonal elements all have values between 0 and 1. If the value is 1 the RD functions are fully correlated and if the value is 0 the RD functions are uncorrelated. Investigation of the shape invariance of RD functions could also lead to the detection of non-linearities or even the identification of non-linear systems, Ibrahim [31], [43] and Haddara [55].

6.2. SYMMETRY TEST

The second approach to quality assessment of the RD functions is based on the symmetry relations for correlation functions of stationary stochastic processes. This approach generally assumes that all possible RD functions are estimated, corresponding to estimating the full correlation matrix of the measurements at each time step. The symmetry relation is

$$R_{YX}(\tau) = R_{XY}(-\tau) \tag{31}$$

If the estimated RD functions are scaled to be equal to the correlation functions (normalized with the triggering levels) then an error and an average function can be defined as

$$\hat{R}^{error}_{YX} = \frac{\hat{R}_{YX}(\tau) - \hat{R}_{XY}(-\tau)}{2} \qquad \hat{R}^{average}_{YX}(\tau) = \frac{\hat{R}_{YX}(\tau) + \hat{R}_{XY}(-\tau)}{2} \tag{32}$$

If the above procedure is applied the number of RD functions is still the same, but there is only an estimate for the positive time lags and the corresponding error function. The quality of the RD functions can now be evaluated by plotting the final RD functions versus the error function. This procedure can also be used to choose the number of points used in the estimation of modal parameters.

6.2. CHOICE OF TRIGGERING LEVELS

One of the difficulties in applications of the RD technique is how to choose the triggering levels $[a_1\ a_2]$ for a given triggering condition. From a user point of view it is important to know how to choose a proper triggering level and to know how sensitive the results are to the choice of triggering level. The optimal choice of triggering level is defined as the choice which minimizes the variance of the RD functions normalized with the triggering level.

$$\min(\mathrm{Var}[\frac{\hat{D}_{XX}(\tau)}{\tilde{a}}]) \rightarrow [a_1\ a_2] \tag{33}$$

For the level triggering condition eq. (33) has been solved. The solution is a triggering level of $a = \sqrt{2}\sigma_X$. This result was derived by Hummelshøj et al. [51]. The assumptions are that the processes are stationary zero mean Gaussian distributed and that the time segments used in the averaging process are independent. The latter assumption is of course violated in some sense. However, the above result is considered to be a good basis for selecting the triggering level for the level crossing triggering condition. The result has been supported by a simulation study, see Brincker et al. [46].

For the local extremum triggering condition an equivalent study can be performed. The variance of the estimated RD functions using the local extremum triggering condition can be approximated by, see Asmussen [72]

$$\mathrm{Var}[\hat{D}_{XX}(\tau)] = \frac{\sigma_X^2}{N}\left(1 - \left(\frac{R_{XX}(\tau)}{\sigma_X^2}\right)^2 - \left(\frac{R'_{XX}(\tau)}{\sigma_X \sigma_{\dot{X}}}\right)^2\right) + \frac{k^E}{N}\left(\frac{R_{XX}(\tau)}{\sigma_X^2}\right)^2 \tag{34}$$

The constant k^E is a function of the triggering levels.

$$k^E = \frac{\int_{a_1}^{a_2} x^2 p_X(x)dx}{\int_{a_1}^{a_2} p_X(x)dx} - \left(\frac{\int_{a_1}^{a_2} x p_X(x)dx}{\int_{a_1}^{a_2} p_X(x)dx}\right)^2 \tag{35}$$

In order to calculate the expected number of triggering points an SDOF system is considered. The system is loaded by white noise. The natural eigenfrequency and the damping ratio are f=1 Hz and ζ=1%. The expected number of triggering points can be calculated using Rice's formula, see Asmussen [72]. The variance of different combinations of the triggering levels $[a_1\ a_2]$ is calculated for each time lag of the correlation functions. The triggering levels which minimize eq. (33) are taken as the optimal choice. The left-hand part of figure 5 shows the optimal upper triggering level and the optimal lower triggering level as a function of the time lag. The theoretical prediction does not take the correlation between the time segments in the averaging process into account. In order to check the above result a simulation study is performed. 500 responses of the SDOF system loaded by Gaussian white noise are simulated. Each time series contains 5000 points and is sampled with 15 Hz. Estimates of the correlation function are calculated for each response using the local extremum triggering condition with different triggering levels. The triggering levels are chosen as all possible combinations of $a_1 = [0, 0.2, ..., 3] \cdot \sigma_X$, $a_2 = [0, 0.2, ..., 3] \cdot \sigma_X$ under the constraint that $a_2 > a_1$. The maximum upper level is chosen as $3\sigma_X$, since it is very unlikely to find realizations of the response beyond $3\sigma_X$. A higher maximum upper level would demand simulation of extremely long time series. A similar argument is used to select the resolution of the triggering levels to 0.2. A higher resolution would also demand simulation of extremely long time series. The optimal triggering levels are chosen as the levels with minimum error calculated as the sum of the absolute values of the difference between the simulated and theoretical correlation functions. The result of the simulation study is shown in the right hand part of figure 5.

The results of fig. 5 show good agreement with the theoretical predictions in fig. 5. It is recommended that the triggering levels for the local extremum triggering condition should be chosen around $[a_1\ a_2] = [\sigma_X\ \infty]$. The best way to select the optimal triggering levels is to perform a sensitivity study. The lower triggering level could be chosen as e.g. $[0\ 0.5\ 1\ 1.5] \cdot \sigma_X$ and the upper triggering level as infinity and the RD functions with lowest errors calculated using the symmetry relations should decide which triggering levels are optimal.

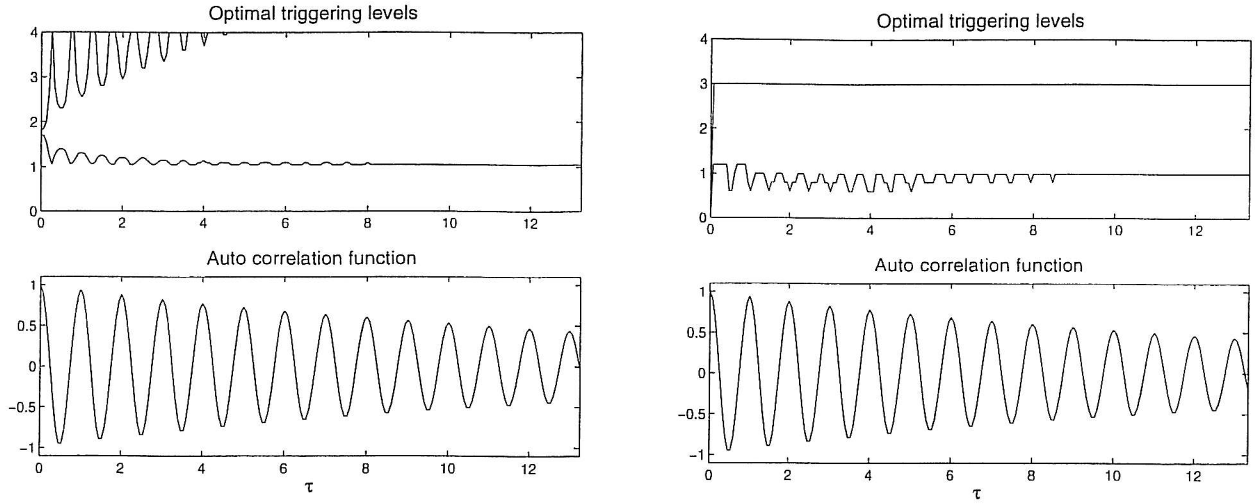

Figure 5: *Theoretically predicted (left-hand part) and simulated (right-hand part) optimal lower and upper triggering level (x) for an SDOF system using local extremum triggering and the corresponding correlation function.*

A simulation study corresponding to the above is performed using the positive point triggering condition. The aim is to investigate how the triggering levels should be chosen. A theoretical prediction can be calculated, but the assumption of uncorrelated time segments is highly violated so the prediction is excluded. The results in fig. 6 indicates that the triggering levels for the positive point triggering condition should be chosen as about $[a_1\ a_2] = [\sigma_X\ \infty]$.

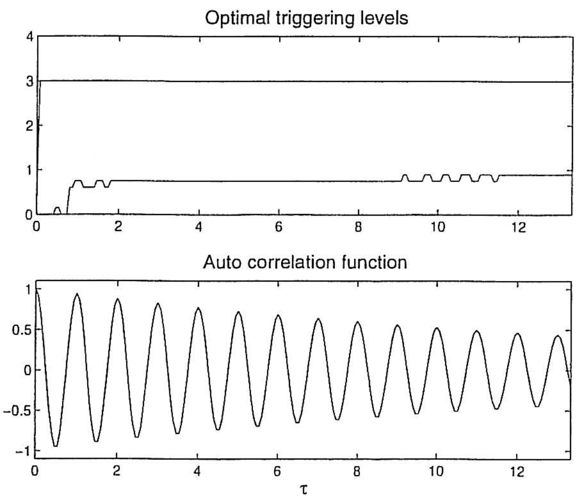

Figure 6: *Optimal triggering levels for positive point triggering for an SDOF system estimated by simulation together with the corresponding correlation function.*

During this section new information how to select the triggering levels for the different triggering conditions is obtained. It is shown that it can be appropriate to exclude the triggering points between 0 and σ_X. Although this is only a guideline it is important new information. The reason is that the accuracy of the estimates is increased and at the same time the estimation time is decreased since triggering points are excluded.

7. EXAMPLE - AMBIENT TESTING OF BRIDGES

In order to illustrate the application of the theory presented in section 5 and suggested in section 6 an analysis of ambient bridge data is performed. The bridge has three spans with 90 m overpass. The deck is a 185 mm thick polypropylene fibre reinforced concrete slab with tension slabs but without any internal steel reinforcement. The bridge and the data collection equipment is described in Ventura et al. [83]. Figure 7 illustrates the bridge and the measurement locations on the bridge.

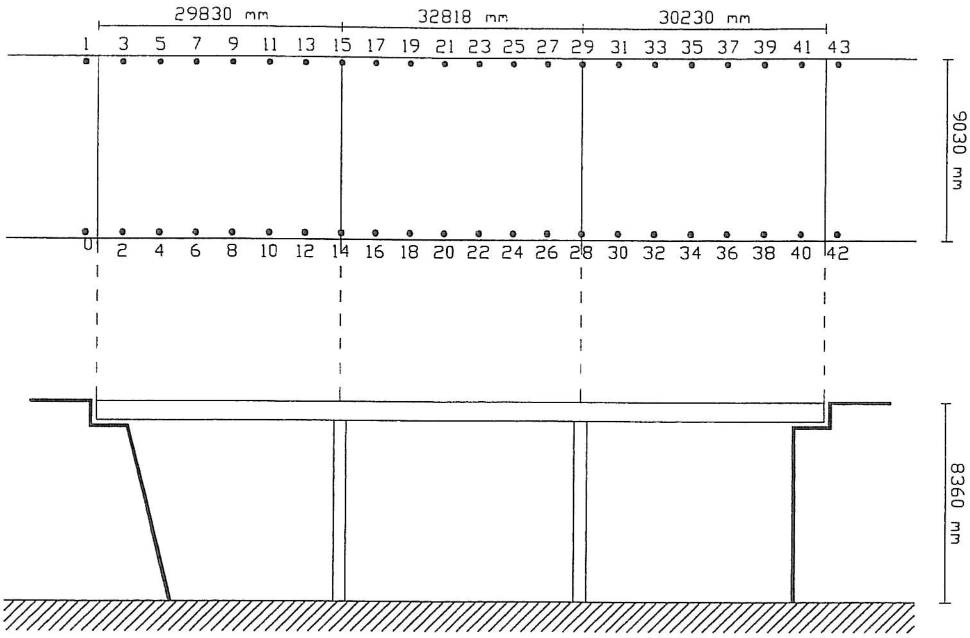

Figure 7: *Outline diagram of the University Drive/Crowchild Trail Bridge.*

The data were sampled at 100 Hz with 65536 points in each measurement. 12 setups each with 8 measurements were collected. In order to limit the number of modes the data are lowpass filtered digitally at 6.25 Hz. It is expected that approximately 6 or seven structural modes are present in the interval 0-6.25 Hz.

Figure 8 shows time and frequency domain plot of the data.

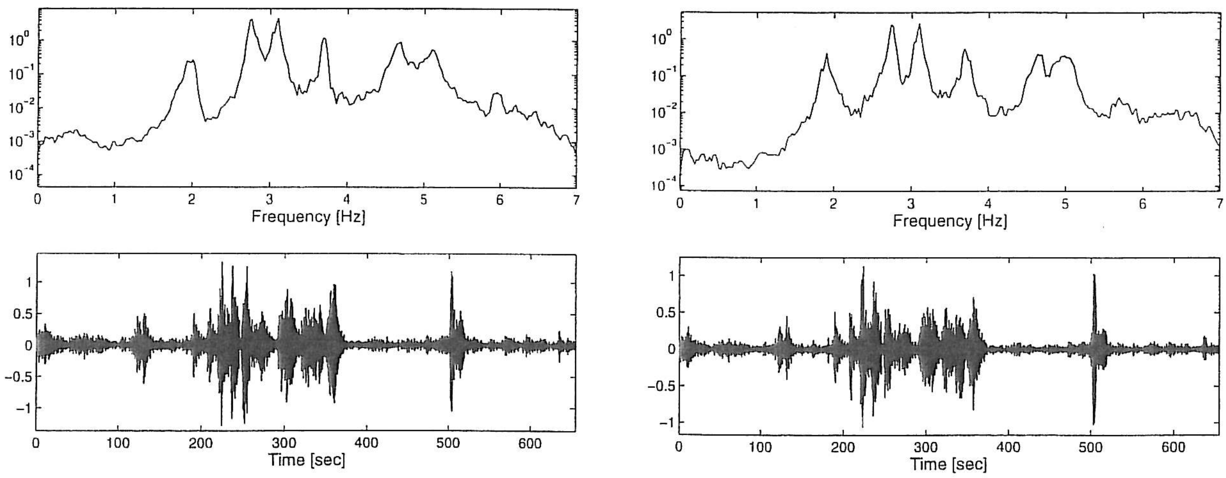

Figure 8: *Time and frequency domain plot of measurement 2 (left) and 5 (right) from setup 2.*

The next step is to perform a pre-analysis or quality assessment of the data for the selection of proper triggering levels and function length. It is chosen to use the banded positive triggering condition. Setup 2 measurement 2 is considered and the function length is chosen to be -10 Hz - 10 Hz. Two different triggering levels are considered: $[a_1\ a_2] = [0\ \infty]$ and $[a_1\ a_2] = [0.5\sigma_X\ \infty]$. The two different RD function are shown in the left-hand side of figure 9. The right hand side of figure 9 shows the average (full line) and error (dotted line - multiplied by 10) of the normalized RD functions.

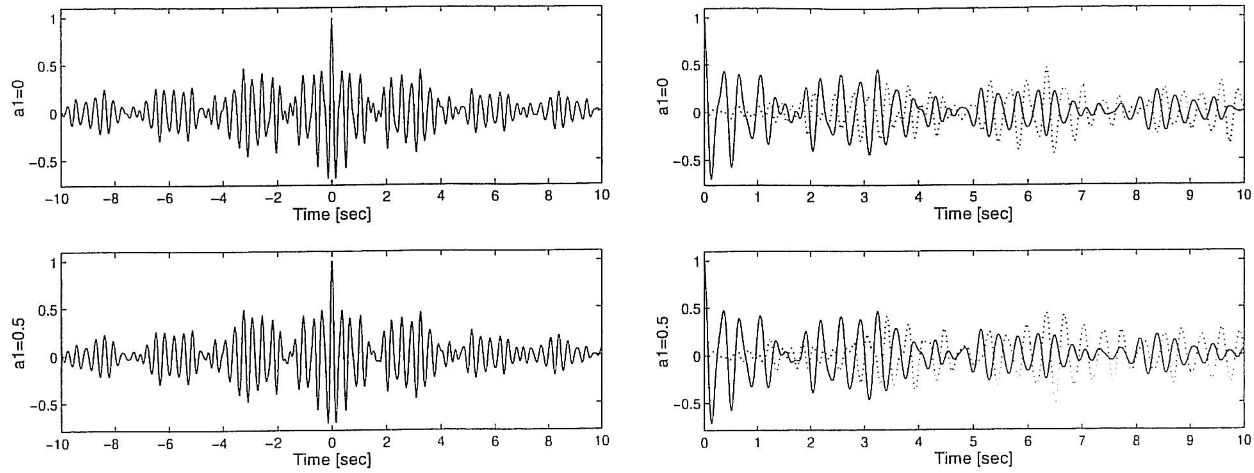

Figure 9: *Full RD functions (left-hand side) and average (full line) and error (dotted line) RD functions (right-hand side).*

It seems that the length of the RD functions is chosen properly. The RD function has decayed and 1000 points are sufficient for modal parameter extraction. Figure 10 shows the shape invariance criteria for setup 4. The lower triggering level is chosen as $a_1 = [0\ 0.25\ 0.5\ 0.75\ 1.00\ 1.25\ 1.5]$ and the upper level is always $a_2 = \infty$. In general there is a high correlation between the different RD functions. If the lower triggering level is chosen in between 0 and $0.75\sigma_X$ it seems that there is nearly always full correlation. This indicates that the lower triggering level should be chosen in between 0 and $0.75\sigma_X$. In this area shape invariance is preserved.

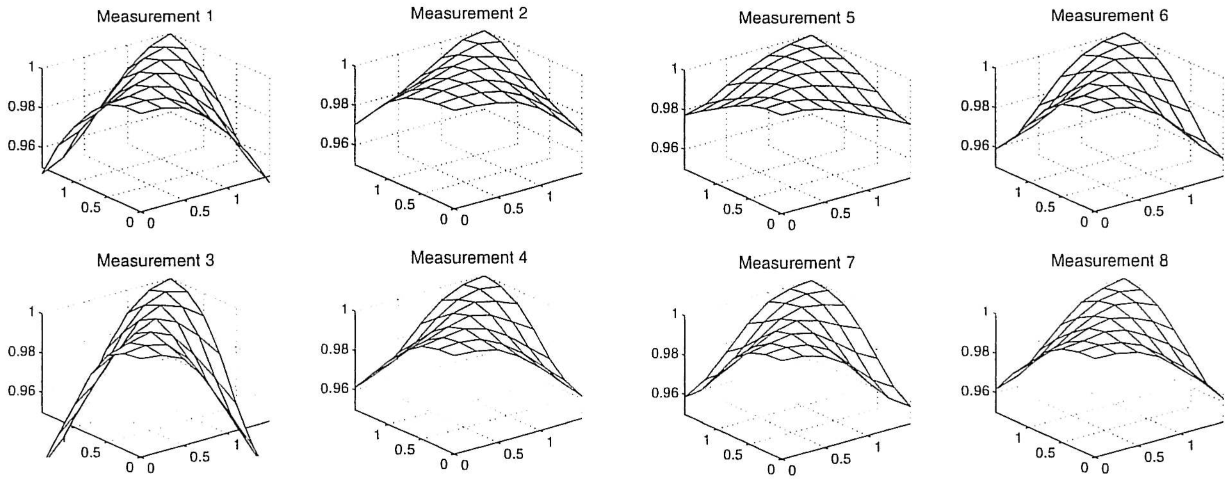

Figure 10: *Shape Invariance criteria for measurements 1-8 from setup 4.*

The symmetry test is considered. The auto RD functions are calculated from all measurements in all setups with a1 varying as $[0\ 0.25\ 0.5\ 0.75\ 1\ 1.25\ 1.25]\sigma_X$ and $a_2 = \infty$. The length of the RD function is $\tau \in [-10; 10]$ Hz. The error measure defined as the RMS of the error function divided by the RMS of the average function (see equation (32)) is calculated. Figure 11 shows the mean value of all error measures for auto RD functions for each setup as a function of the lower triggering level. The overall conclusion of this investigation is that the lower triggering level should be chosen in between $[0.5\sigma_X\ \sigma_X]$. In order to minimize the number of triggering points the triggering is chosen as $[a_1\ a_2] = [\sigma_X\ \infty]$. To extract maximum information $[a_1\ a_2] = [-\sigma_X\ \ -\infty]$ is also applied. Using these triggering levels the full RD matrix is calculated for all 12 setups.

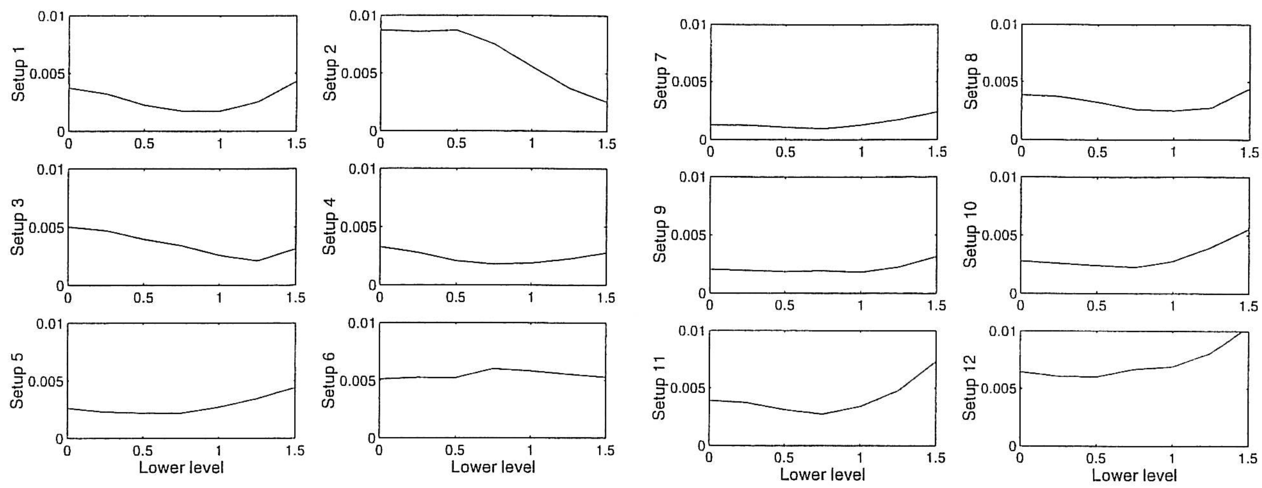

Figure 11: *Mean value of the quality measure for the different setups.*

To have an idea about the number of modes present in the RD functions an average spectral density function is calculated. All RD functions are Fourier transformed and averaged. The absolute value of this function is seen in fig. 12. The spikes indicate structural modes. As indicated there could be structural modes at the following frequencies [1.85 2.78 3.13 3.76 4.05 4.17 4.64 5.18] Hz.

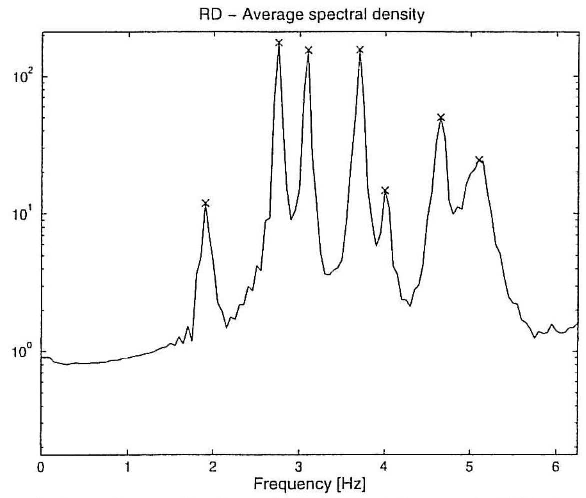

Figure 12: *Average spectral density calculated from estimated RD functions and expected structural modes.*

The Polyreference Time Domain (PTD) technique is applied to the averaged RD functions from each setup. Figure 13 show the results from all setups where 30 and 35 modes and 500 and 600 points are used as input to PTD for each setup.

The following modes could be estimated for all setups

f [Hz]	2.75	3.09	3.72	4.65	5.15
ζ [%]	0.85	0.93	1.80	1.24	2.08

As seen there is also a mode present at 4.05 Hz at several of the setups.

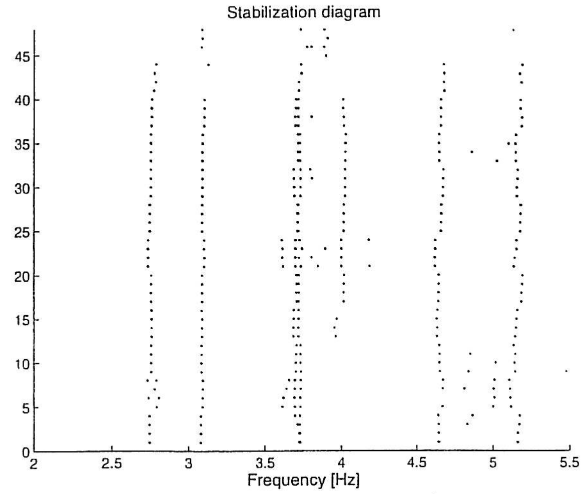

Figure 13: *Stabilization diagram.*

The mode shapes corresponding to the 4 lowest modes are shown in fig. 14

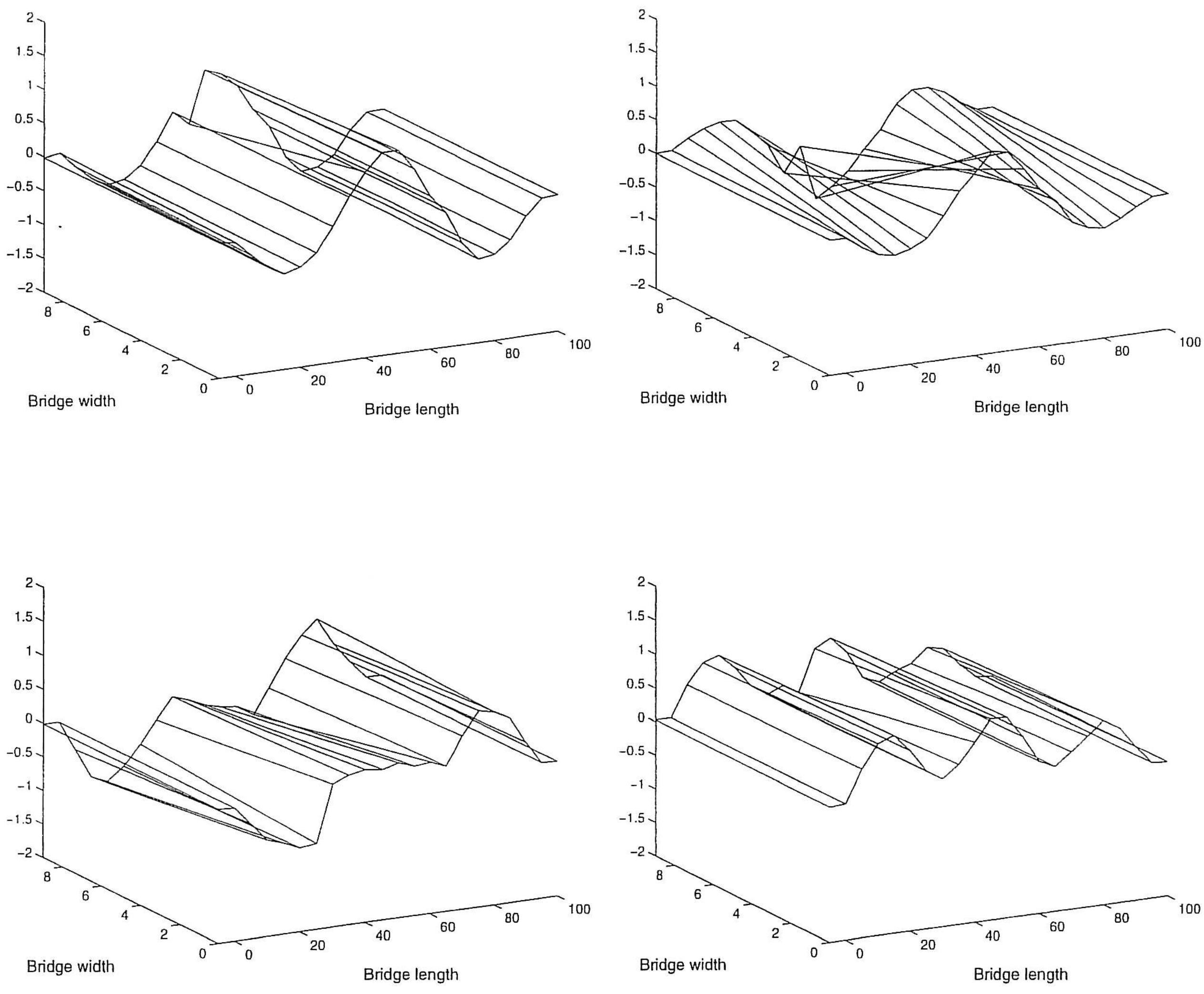

Figure 14: *Mode shape estimates from the 4 lowest modes of the bridge.*

8. VECTOR TRIGGERING RANDOM DECREMENT

The Vector Random Decrement (VRD) technique was introduced as an efficient alternative to the traditional RD technique. If e.g. 8 or 16 measurement are collected simultaneously, it can be tedious to estimate all 64 or 256 RD functions. Instead only a few columns of the RD matrix are estimated, which limits the information available. The problem is how to choose these columns. These problems motivated the development of the VRD technique, see references [69,70,73,79].

Consider a stationary stochastic vector process $\mathbf{X}(t) = [X_1(t)\ X_2(t)\ X_3(t)\ \dots\ X_k(t)\ X_{k+1}(t)\ \dots\ X_l(t)\ X_{l+1}(t)\ \dots\ X_n(t)]^T$. The VRD functions are defined as

$$\mathbf{D}_{\mathbf{X}X_{k,l}}(\tau) = \mathrm{E}[\mathbf{X}(t+\tau)|T^v_{X_{k,l}(t+\Delta t)}] \tag{36}$$

where the vector triggering condition is given by

$$\begin{aligned} T^v_{X_{k,l}(t+\Delta t)} &= T^v_{X_k(t+\Delta t_k), X_{k+1}(t+\Delta t_{k+1}), \dots X_l(t+\Delta t_l)} \quad , \quad 2 \leq k < l \leq n \\ &= \{a_k \leq X_k(t+\Delta t_k) \leq b_k,\ \dots\ , a_l \leq X_l(t+\Delta t_l) \leq b_l\} \end{aligned} \tag{37}$$

Using this vector condition and assuming that $\mathbf{X}(t)$ is Gaussian distributed, it can be proven, see Asmussen [72,79], that the resulting VRD functions are given by

$$\mathbf{D}^v_X(\tau) = \mathbf{R}_{X_k}(\tau - \Delta t_k) \cdot a_k + \mathbf{R}_{X_{k+1}}(\tau - \Delta t_{k+1}) \cdot a_{k+1} + \dots + \mathbf{R}_{X_l}(\tau - \Delta t_l) \cdot a_l \tag{38}$$

where the constants a_i depend on the covariance matrix of $\mathbf{X}(t)$ and the triggering levels in equation (37). $\mathbf{R}_{X_k}(\tau - \Delta t_k)$ is the kth column of the correlation matrix of $\mathbf{X}(t)$ at time lag $\tau - \Delta t_k$. As seen from the results of equation (38) the advantage of the VRD technique is that information from the full correlation matrix can be obtained from a single estimation. This is not possible for the RD technique or an algorithm based on FFT. Several examples on the VRD technique applied to real and simulated data are given in references [69,70,73,79].

9. CONCLUSIONS

The RD transform has been described from its introduction to the most recent developments. To support the brief review a detailed bibiliography is given. The RD functions are defined as conditional mean values and can be unbiased estimated provided that the considered processes are ergodic. A new approach to estimate the frequency response functions of linear systems based on the RD technique is suggested and a simple example is given. Using a generalized condition a relation between the RD functions and the correlation functions of jointly distributed Gaussian processes is described. From this relation a new approach for quality assessment is suggested. The purpose is to have a standardized method to select the triggering levels and function length of the RD functions. This issue is illustrated by the analysis of ambient bridge data. The paper is finished with a short description of the most recent development, the vector RD technique.

ACKNOWLEDGEMENT

Financial support from the Danish Technical Research Council is acknowledged. The access to the high-quality ambient data from the University Drive/Crowchild Bridge collected by Dr. Ventura and coworkers (see reference [83]) is highly appreciated.

REFERENCES

[1] H.A. Cole 1968 *AIAA Paper No. 68-288.* On-The-Line Analysis of Random Vibrations.

[2] H.A. Cole 1971 *United States Patent No. 3, 620,069.* Method and Apparatus for Measuring the Damping Characteristics of a Structure.

[3] H.A. Cole 1971 *NASA TMX-62,041.* Failure Detection of a Space Shuttle Wing by Random Decrement.

[4] H.A. Cole 1973 *NASA CR-2205* On-Line Failure Detection and Damping Measurements of Aerospace Structures By Random Decrement Signature.

[5] C.S. Chang 1975 *NASA-CR-132563.* Study of Dynamic Characteristics of Aeroelastic Systems Utilizing Randomdec Signatures.

[6] J.C. Houbolt 1975 *Proceedings NASA Symposium on Flutter Testing Techniques NASA SP-415, pp. 1-41.* On Identifying Frequencies and Damping in Subcritical Flutter Testing.

[7] R.M. Bennet & R.N. Desmarais 1975 *Proceedings NASA Symposium on Flutter Testing Techniques NASA SP-415, pp. 43-57.* Curve Fitting of Aeroelastic Transient Response Data with Exponential Functions.

[8] C.E. Hammond & R.V. Dogget 1975 *Proceedings NASA Symposium on Flutter Testing Techniques NASA SP-415, pp. 59-76.* Determination of Subcritical Damping by Moving Block/Randomdec Applications.

[9] L.J. Huttsell & T.E. Noll 1975 *Proceedings NASA Symposium on Flutter Testing Techniques NASA SP-415, pp. 193-211.* Wind Tunnel Investigation of Supersonic Wing-Tail Flutter.

[10] R.W. Lenz & B. McKeever 1975 *Proceedings NASA Symposium on Flutter Testing Techniques NASA SP-415, pp. 287-317.* Time Series Analysis in Flight Flutter Testing at the Air Force Flight Test Center: Concepts and Results.

[11] H.J. Perangelo & F.W. Milordi 1975 *Proceedings NASA Symposium on Flutter Testing Techniques NASA SP-415, pp. 319-375.* Flight Flutter Testing Technology at Grumman.

[12] M.A. Abla 1975 *Proceedings NASA Symposium on Flutter Testing Techniques NASA SP-415, pp. 395-411.* The Application of Recent Techniques in Flight Flutter Testing.

[13] W.J. Brignac, H.B. Ness, M.K. Johnson & L.M. Smith 1975 *Proceedings NASA Symposium on Flutter Testing Techniques NASA SP-415, pp. 433-457.* YF-16 Flight Flutter Test Procedures.

[14] R.E. Reed & H.A. Cole 1975 *NASA CR-137609.* Applicability of Randomdec Technique to Flight Simulator for Advanced Aircraft.

[15] J.C.S. Yang & D.W. Caldwell 1975 *46th Shock and Vibration Symposium and Bulletin.* The Measurement of Damping and the Detection of Damages in Structures by the Random Decrement Technique.

[16] S.R. Ibrahim 1977 *Journal of Spacecraft and Rockets, Vol. 14, No. 11, pp. 696-700.* Random Decrement Technique for Modal Identification of Structures.

[17] S.R. Ibrahim 1977 *AIAA paper, Vol. 77, pp. 1-9.* The Use of Random Decrement Technique for Identification of Structural Modes of Vibration.

[18] Yang, J.C.S. & Caldwell, D.W. 1978 *ASME Probabilistic Analysis and Design of Nuclear Power Plant Structures Manual PVB-PB-030, 1978, pp. 97-117.* A Method for Detecting Structural Deterioration in Piping Systems.

[19] Caldwell, D.W. 1978 *Ph.D.-Thesis, University of Maryland.* The Measurement of Damping and the Detection of Damage in Linear and Nonlinear Systems by the Random Decrement Technique.

[20] Reed, R.E. 1979 *AIAA/ASME/AHS 20th Structures, Structural Dynamics and Materials Conference. pp. 404-409.* Analytical Aspects of Randomdec Analysis.

[21] Ibrahim, S.R. 1979 *The Shock and Vibration Bulletin, Bulletin 49, Part 2 of 3, pp. 165-170.* Application of Random Time Domain Analysis to Dynamic Flight Measurements.

[22] Ibrahim, S.R. 1980 *The Shock and Vibration Bulletin. Bulletin 50 (Part 3 of 4). Dynamic Analysis, Design Techniques, pp. 99-112.* Limitations on Random Input Forces in Randomdec Computation for Modal Identification.

[23] Yang, J.C.S., Dagalakis, N. & Hirt, M. 1980 *Computer Methods for Offshore Structures. Winter Annual Meeting of ASME, pp. 55-67.* Application of the Random Decrement Technique in the Detection of an Induced Crack on an Offshore Platform Model.

[24] Kummer, E., Yang, J.C.S. & Dagalakis, N. 1981 *Proceedings 2nd ASCE/EMD Specialty Conference on Dynamic Response of Structures. pp. 445-460.* Detection of Fatigue Cracks in Structural Members.

[25] Yang, J.C.S., Aggour, M.S., Dagalakis, N. & Miller, F. 1981 *Proceedings 2nd ASCE/EMD Specialty Conference on Dynamic Response of Structures. pp. 819-832.* Damping of an Offshore Platform Model by Random Dec Method.

[26] J. Nasir & S.S. Sunder 1982 *Massachussetts Institute of Technology, Department of Civil Engineering, Research Report R82-52.* Evaluation of the Random Decrement Technique of Vibration Signature Analysis for Monitoring of Offshore Platforms.

[27] J.K. Vandiver, A.B. Dunwoody, R.B. Campbell & M.F. Cook 1982 *Journal of Mechanical Design, Vol. 104, pp. 307-313.* A Mathematical Basis for the Random Decrement Vibration Signature Analysis Technique.

[28] Kiraly, L.J. 1982 *NASA Technical Memorandum 82853, NASA-TA-82853. (Prepared for the 1982 Aerospace/Test Measurement Symposium.)* A High Speed Implementation of the Random Decrement Algorithm.

[29] Huan,S.-L., McInnis, B.C. & Denman, E.D. 1983 *International Journal of Systems Science, Vol. 14, No. 4, 417-423.* Analysis of the Random Decrement Method.

[30] J.C.S. Yang, J. Chen, & N. Dagalakis 1984 *ASME, Journal of Energy Resources Technology, Vol. 106, pp. 38-42.* Damage Detection in Offshore Structures by the Random Decrement Technique.

[31] S.R. Ibrahim. 1984 *AIAA Journal, Vol. 6, No. 6, June, 1984, pp. 817-823.* Time-Domain Quasilinear Identification of Nonlinear Dynamic Systems.

[32] T. Tsai, J.C.S. Yang & R.Z. Chen 1985 *Proc. 3rd International Modal Analysis Conference, Orlando, Florida, pp. 691-700.* Detection of Damages in Structures by the Cross Random Decrement Technique.

[33] J.C.S. Yang, T. Tsai, W.H. Tsai & Z. Chen 1985 *Proc. 4th Internatianal Offshore Mechanics and Arctic Engineering Symposium, Dallas, Texas, pp. 496-504.* Detection and Identification of Structural Damage from Dynamic Response Measurements.

[34] J.C.S. Yang, T. Tsai, V. Pavlin, J. Chen, & W.H. Tsai 1985 *The Shock and Vibration Bulletin, Bulletin 55, Part 3 in 5, pp. 57-66.* Structural Damage Detection by the System Identification Technique.

[35] J.C.S. Yang, C.H. Marks, J. Jiang, D. Chen, A. Elahi, & W.-H. Tsai 1985 *ASME Journal of Energy Resources Technology, Vol. 107 pp. 220-225.* Determination of Fluid Damping using Random Excitation.

[36] R. Siviter & M.G. Pollard 1985 *Vehicle Systems Dynamics, Vol. 14. No. 1-3 June 1985, pp. 136-140.* Measurement of Railway Vehicle Kinematic Behaviour using the Random Decrement Technique.

[37] H.A. Al-Sannad, M.S. Aggour & M.I. Amer 1986 *Indian Geotechnical Journal, Vol. 16, No. 2, pp. 126-135* Use of Random Loading in Soil Testing.

[38] S.R. Ibrahim 1986 *The International Journal of Analytical and Experimental Modal Analysis. Vol. 1, No. 2, pp. 1-9.* Incipient Failure Detection from Random-Decrement Time Functions.

[39] N.E. Bedewi 1986 *Ph.D.-Dissertation, University of Maryland, 1986.* The Mathematical Foundation of the Auto and Cross Random Decrement Technique and the Development of a System Identification Technique for Detection of Structural Deterioration.

[40] N.E. Bedewi, D.-N. Kung, G.Z. Qi, & J.C.S. Yang 1987 *Proc. Nondestructive Testing of High-Performance Ceramics, Boston, MA, USA, pp. 424-441.* Use of the Random Decrement Technique for Detecting Flaws and Monitoring the Initiation and Propagation of Fatigue Cracks in High-Performance Materials.

[41] N.E. Bedewi & J.C.S. Yang 1987 *Proceedings 58th Shock and Vibration Symposium, Vol.1 pp. 257-273.* A System Identification Technique Based on the Random Decrement Signatures. Part 1: Theory and Simulation.

[42] Bedewi, N.E. & Yang, J.C.S. 1987 *Proceedings 58th Shock and Vibration Symposium, Vol.1 pp. 275-287.* A System Identification Technique Based on the Random Decrement Signatures. Part 2: Experimental Results.

[43] S.R. Ibrahim, K.R. Wentz & J. Lee 1987 *Mechanical Systems and Signal Processing (1987) 1(4), pp 389-397.* Damping Identification from Non-Linear Random Responses using a Multi-Triggering Random Decrement Technique.

[44] D.-N. Kung, G.-Z- Qi, J.C.S. Yang & N. Bedewi. 1988 *Proceedings 6th International Modal Analysis Conference, pp. 350-356.* Fatique Life Characterization of Composite Structures using the Random Decrement Modal Analysis Technique.

[45] P. Bernard 1988 *Journal of Theoretical and Applied Mechanics. Vol. 7, No. 3, 1988, pp. 269-280. (In French).* Identification de Grandes Structures: Une Remarque sur la Méethode du Décrement Aléatoire.

[46] R. Brincker, S. Krenk & J.L. Jensen 1990 *Proc. Skandinavisk Forum for Stokastisk Mekanik, Lund, Sweden.* Estimation of Correlation Functions by the Random Dec Technique.

[47] N.E. Bedewi & J.C.S. Yang 1990 *Proceedings ASME International Conference and Exposition, pp. 195-201.* The Random Decrement Technique: A More Efficient Estimator of the Correlation Function.

[48] R. Brincker, J.L. Jensen& S. Krenk 1990 *Proceedings 9th International Conference on Experimental Mechanics.* Spectral Estimation by the Random Dec Technique.

[49] J.C.S. Yang, G.Z. Qi& C.D. Kan 1990 *Proceedings 8th International Modal Analysis Conference, pp. 28-34.* Mathematical Base of Random Decrement Technique.

[50] N.E. Bedewi & J.C.S. Yang 1990 *Proceedings 1990 ASME International Comp. In Engineering Conference and Exposition, pp. 77-86.* The Relationship Between the Random Decrement Signature and the Free Decay Response of Multidegree-Of-Freedom Systems.

[51] L.G. Hummelshøj, H. Møller & L. Pedersen 1991 *M.Sc.-thesis Aalborg University.* Skadesdetektering ved respons måling (in danish).

[52] R. Brincker, P.H. Kirkegaard & A. Rytter 1991 *Proceedings 16th International Seminar on Modal Analysis.* Identification of System Parameters by the Random Decrement Technique.

[53] R. Brincker, S. Krenk & J.L. Jensen 1991 *Proc. 9th International Modal Analysis Conference and Exhibit, Firenze, Italy.* Estimation of Correlation Functions by the Random Decrement Technique.

[54] H.G. Natke 1992 *3rd Edition, Vieweg, Braunschweig.* Einführung in Theorie und Praxis der Zeitreihen- und Modalanalyse-Identifikation schwingungsfähiger elastomechanischer Systeme.

[55] M.R. Haddara 1992 *OMAE, Vol. 2, Safety and Reliability, ASME 1992, pp. 321-324.* On the Random Decrement for Nonlinear Rolling Motion.

[56] R. Brincker, S. Krenk, P.H. Kirkegaard & A. Rytter 1992 *Bygningsstatiske Meddelelser, Vol. 63, No. 1, pp. 1-38.* Identification of Dynamical Properties from Correlation Function Estimates.

[57] M. Bodruzzaman, X. Li, C. Wang & S. Devgan 1993 *Souteastcon '93.* Identifying Modes of Vibratory System Excited by Narrow Band Random Excitations.

[58] Y. Tamura, A. Sasaki & H. Tsukagoshi 1993 *Journal of Structural and Construction Engineering, AIJ, No. 454, Dec. 1993. (In Japanese) Evaluation of Damping Ratios of Randomly Excited Buildings Using the Random Decrement Technique.*

[59] R. Brincker, M. Demosthenous & G.C. Manos 1994 *Proceedings 12th International Modal Analysis Conference.* Estimation of the Coefficient of Restitution of Rocking Systems by the Random Decrement Technique.

[60] M.J. Desforges, J.E. Cooper & J.R. Wright. 1995 *Journal of Mechanical Systems and Signal Processing, Vol 9, No. 2, pp. 169-186.* Spectral and Modal Parameter Estimation From Output-Only Measurements.

[61] J.C. Asmussen & R. Brincker 1996 *Proceedings 14th International Modal Analysis Conference, Vol I, pp. 246-252.* Estimation of Frequency Response Functions by Random Decrement.

[62] S.R. Ibrahim, J.C. Asmussen & R. Brincker. 1996 *Proceedings 14th International Modal Analysis Conference, Vol I, pp. 446-452.* Modal Parameter Identification from Responses of General Unkonwn Random Inputs.

[63] J.C. Asmussen, S.R. Ibrahim & R. Brincker 1996 *Proceedings 14th International Modal Analysis Conference, Vol I, pp. 453-458.* Random Decrement and Regression Analysis of Traffic Responses of Bridges.

[64] J.C. Asmussen & R. Brincker 1996 *Proceedings ISMA21 - Noise and Vibration Engineering, Vol II, pp. 1215-1224.* Estimation of Correlation Functions by Random Decrement.

[65] P.D. Spanos & B.A. Zeldin 1996 *Proceedings 1996 ASCE Specialty Conference on Probabilistic Mechanics and Structural Reliability, pp. 850-853.* Generalized Random Decrement Method for System Identification.

[66] T.J. Chalko & N. Haritos 1997 *Proceedings 15th International Modal Analysis Conference, Vol. I, pp. 13-19.* Scaling Eigenvectors obtained from Ambient Excitation Modal Testing.

[67] A. Fasana L. Garibaldi, E. Giorcelli, M. Ruzzene & D. Sabia 1997 *Proceedings 15th International Modal Analysis Conference, Vol. I, pp. 293-300.* Analysis of a Motorway Bridge Under Random Traffic Excitation.

[68] R. Brincker & J.C. Asmussen 1997 *Proceedings 15th International Modal Analysis Conference, Vol. II, pp. 1571-1576.* Random Decrement Based FRF Estimation.

[69] S.R. Ibrahim, J.C. Asmussen & R. Brincker 1997 *Proceedings 15th International Modal Analysis Conference, Vol. I, pp. 502-509.* Theory of Vector Triggering Random Decrement.

[70] J.C. Asmussen, S.R. Ibrahim & R. Brincker. 1997 *Proceedings 15th International Modal Analysis Conference, Vol. II pp. 1165-1171.* Application of Vector Triggering Random Decrement.

[71] P. Bonato, R. Ceravolo & A. De Stefano 1997 *Journal of Engineering Mechanics Vol. 123 No. 12, pp. 1260-1267.* Time-Frequency and Ambiguity Function Approaches in Structural Identification.

[72] J.C. Asmussen 1997 *Ph.D.-Thesis Aalborg University, Denmark.* Modal Analysis Based on the Random Decrement Technique - Applications to Civil Enginering Structures.

[73] S.R. Ibrahim, J.C. Asmussen & R. Brincker 1997 *Accepted for publication in Journal of Vibration and Acoustics.* Vector Triggering Random Decrement for High Identification Accuracy.

[74] M. Ruzzene, A. Fasana, L. Garibaldi & B. Piombo 1997 *Mechanical Systems and Signal Processing* **11***(2) pp. 207-218.* Natural Frequencies and Dampings Identification Using Wavelet Transform: Application to Real Data.

[75] J.C. Asmussen & R. Brincker 1998 *Proceedings 16th International Modal Analysis Conference, 1998, Vol I, pp. 542-548* A New Approach for Predicting the Variance of Random Decrement Functions.

[76] J.C. Asmussen, S.R. Ibrahim & R. Brincker 1998 *Proceedings 16th International Modal Analysis Conference, 1998, Vol I, pp. 914-921* Random Decrement: Identification of Structures Subjected to Ambient Excitation.

[77] J.C. Asmussen, S.R. Ibrahim & R. Brincker 1998 *Proceedings 16th International Modal Analysis Conference, 1998, Vol I, pp. 922-928* Ambient Vibration Testing of the Vestvej Bridge.

[78] J.C. Asmussen & R. Brincker 1997 *Submitted to Journal of Mechanical Systems and Signal Processing.* A New Approach for Predicting the Variance of Random Decrement Functions.

[79] J.C. Asmussen, S.R. Ibrahim & R. Brincker 1998 *Submitted to Journal of Sound and Vibration.* Statistical Theory of the Vector Random Decrement Technique.

[80] R. Brincker & J.C. Asmussen 1998 *Submitted to Journal of Sound and Vibration* Theory of the Random Decrement Technique.

[81] C.R. Farrar & G.H. James III 1997 *Journal of Sound and Vibration,* **205***(1), pp. 1-18.* System Identification from Ambient Vibration Measurements on a Bridge.

[82] G.H. James III, T.G. Carne & J.P. Lauffer 1995 *Modal Analysis* **10***, pp. 260-277.* The Natural Excitation Technique (NEXT) for Modal Parameter Extraction from Operating Structures.

[83] C.E. Ventura, C. Black and P.-C. Tsai 1997 *Report EQ 97-005 for ISIS Canada prepared at University of British Columbia, Canada.* Ambient Vibration Measurements of the University Drive/Crowchild Trail Bridge in Calgary, Alberta.

FRACTURE AND DYNAMICS PAPERS

PAPER NO. 78: P. Andersen, P. H. Kirkegaard, R. Brincker: *System Identification of Civil Engineering Structures using State Space and ARMAV Models.* ISSN 1395-7953 R9618.

PAPER NO. 79: P. H. Kirkegaard, P. S. Skjærbæk, P. Andersen: *Identification of Time Varying Civil Engineering Structures using Multivariate Recursive Time Domain Models.* ISSN 1395-7953 R9619.

PAPER NO. 80: J. C. Asmussen, R. Brincker: *Estimation of Correlation Functions by Random Decrement.* ISSN 1395-7953 R9624.

PAPER NO. 81: M. S. Henriksen, J. P. Ulfkjær, R. Brincker: *Scale Effects and Transitional Failure Phenomena of Reinforced concrete Beams in Flexure. Part 1.* ISSN 1395-7953 R9628.

PAPER NO. 82: P. Andersen, P. H. Kirkegaard, R. Brincker: *Filtering out Environmental Effects in Damage Detection of Civil Engineering Structures.* ISSN 1395-7953 R9633.

PAPER NO. 83: P. S. Skjærbæk, S. R. K. Nielsen, P. H. Kirkegaard, A. Ş. Çakmak: *Case Study of Local Damage Indicators for a 2-Bay, 6-Storey RC-Frame subject to Earthquakes.* ISSN 1395-7953 R9639.

PAPER NO. 84: P. S. Skjærbæk, S. R. K. Nielsen, P. H. Kirkegaard, A. Ş. Çakmak: *Modal Identification of a Time-Invariant 6-Storey Model Test RC-Frame from Free Decay Tests using Multi-Variate Models.* ISSN 1395-7953 R9640.

PAPER NO. 85: P. H. Kirkegaard, P. S. Skjærbæk, S. R. K. Nielsen: *Identification Report: Earthquake Tests on 2-Bay, 6-Storey Scale 1:5 RC-Frames.* ISSN 1395-7953 R9703.

PAPER NO. 86: P. S. Skjærbæk, S. R. K. Nielsen, P. H. Kirkegaard: *Earthquake Tests on Scale 1:5 RC-Frames.* ISSN 1395-7953 R9713.

PAPER NO. 87: P. S. Skjærbæk, S. R. K. Nielsen, P. H. Kirkegaard, A. Ş. Çakmak: *Experimental Study of Damage Indicators for a 2-Bay, 6-Storey RC-Frame.* ISSN 1395-7953 R9725.

PAPER NO. 88: P. S. Skjærbæk, S. R. K. Nielsen, P. H. Kirkegaard, A. Ş. Çakmak: *Damage Localization and Quantification of Earthquake Excited RC-Frames.* ISSN 1395-7953 R9726.

PAPER NO. 89: P. S. Skjærbæk, P. H. Kirkegaard, S. R. K. Nielsen: *Shaking Table Tests of Reinforced Concrete Frames.* ISSN 1395-7953 R9704.

PAPER NO. 90: P. H. Kirkegaard, P. Andersen: *Use of Statistical Information for Damage Assessment of Civil Engineering Structures.* ISSN 1395-7953 R9723.

PAPER NO. 91: P. S. Skjærbæk, P. H. Kirkegaard, G. N. Fouskitakis, S. D. Fassois: *Non-Stationary Modelling and Simulation of Near-Source Earthquake Ground Motion: ARMA and Neural Network Methods.* ISSN 1395-7953 R9641.

PAPER NO. 92: J. C. Asmussen, S. R. Ibrahim, R. Brincker: *Application of Vector Triggering Random Decrement.* ISSN 1395-7953 R9634.

PAPER NO. 93: S. R. Ibrahim, J. C. Asmussen, R. Brincker: *Theory of Vector Triggering Random Decrement.* ISSN 1395-7953 R9635.

FRACTURE AND DYNAMICS PAPERS

PAPER NO. 94: R. Brincker, J. C. Asmussen: *Random Decrement Based FRF Estimation.* ISSN 1395-7953 R9636.

PAPER NO. 95: P. H. Kirkegaard, P. Andersen, R. Brincker: *Structural Time Domain Identification (STDI) Toolbox for Use with MATLAB.* ISSN 1395-7953 R9642.

PAPER NO. 96: P. H. Kirkegaard, P. Andersen: *State Space Identification of Civil Engineering Structures from Output Measurements.* ISSN 1395-7953 R9643.

PAPER NO. 97: P. Andersen, P. H. Kirkegaard, R. Brincker: *Structural Time Domain Identification Toolbox - for Use with MATLAB.* ISSN 1395-7953 R9701.

PAPER NO. 98: P. S. Skjærbæk, B. Taşkin, S. R. K. Nielsen, P. H. Kirkegaard: *An Experimental Study of a Midbroken 2-Bay, 6-Storey Reinforced Concrete Frame subject to Earthquakes.* ISSN 1395-7953 R9706.

PAPER NO. 99: P. S. Skjærbæk, S. R. K. Nielsen, P. H. Kirkegaard, B. Taşkin: *Earthquake Tests on Midbroken Scale 1:5 Reinforced Concrete Frames.* ISSN 1395-7953 R9712.

PAPER NO. 100: J. C. Asmussen: *Modal Analysis based on the Random Decrement Technique. Application to Civil Engineering Structures.* Ph.D.-Thesis. ISSN 1395-7953 R9753.

PAPER NO. 101: P. Andersen: *Identification of Civil Engineering Structures using Vector ARMA Models.* Ph.D. Thesis. ISSN 1395-7953 R9724.

PAPER NO. 102: J. C. Asmussen, R. Brincker, A. Rytter: *Ambient Modal Testing of the Vestvej Bridge using Random Decrement.* ISSN 1397-7953 R9731.

PAPER NO. 103: J. C. Asmussen, R. Brincker: *A New Approach for Predicting the Variance of Random Decrement Functions.* ISSN 1397-7953 R9733.

PAPER NO. 104: P. H. Kirkegaard, L. Pilegaard Hansen: *Cable Dynamics - A Literature Review.* ISSN 1395-7953 R9813.

PAPER NO. 105: P. H. Kirkegaard, L. Pilegaard Hansen: *Vibration Measurements on the Frejlev Mast.* ISSN 1395-7953 R9814.

PAPER NO. 106: P. H. Kirkegaard, L. Pilegaard Hansen: *Estimation of Cable Forces of a Guyed Mast from Dynamic Measurements.* ISSN 1395-7953 R9815.

PAPER NO. 107: P. Andersen, P. H. Kirkegaard: *Statistical Damage Detection of CivilEngineering Structures using ARMAV Models.* ISSN 1395-7953 R9758.

PAPER NO. 108: P. Andersen: *Estimation of Modal Parameters and their Uncertainties.* ISSN 1395-7953 R9816.

PAPER NO. 109: J. C. Asmussen, S. R. Ibrahim, R. Brincker: *Random Decrement: Identification of Structures subjected to Ambient Excitations.* ISSN 1395-7953 R9759.

PAPER NO. 110: J. C. Asmussen, R. Brincker, S. R. Ibrahim: *Modal Analysis based on The Random Decrement Transform.* ISSN 1395-7953 R9821.

Department of Building Technology and Structural Engineering
Aalborg University, Sohngaardsholmsvej 57, DK 9000 Aalborg
Telephone: +45 9635 8080 Telefax: +45 9814 8243